

Retrievals of profiles of fine and coarse aerosols using lidar and radiometric space measurements

Submitted to IEEE: TGRS-00230-2002

Yoram Kaufman¹, Didier Tanré,² Jean-François Léon² and Jacques Pelon³

Abstract

In couple of years we expect the launch of the CALIPSO lidar spaceborne mission designed to observe aerosols and clouds. CALIPSO will collect profiles of the lidar attenuated backscattering coefficients in two spectral wavelengths (0.53 and 1.06 μm). Observations are provided along the track of the satellite around the globe from pole to pole. The attenuated backscattering coefficients are sensitive to the vertical distribution of aerosol particles, their shape and size. However the information is insufficient to be mapped into unique aerosol physical properties and vertical distribution. Infinite number of physical solutions can reconstruct the same two wavelength backscattered profile measured from space. CALIPSO will fly in formation with the Aqua satellite and the MODIS spectro-radiometer on board. Spectral radiances measured by MODIS in six channels between 0.55 and 2.13 μm simultaneously with the CALIPSO observations can constrain the solutions and resolve this ambiguity, albeit under some assumptions. In this paper we describe the inversion method and apply it to aircraft lidar and MODIS data collected over a dust storm off the coast of West Africa during the SHADE

¹ NASA Goddard Space Flight Center, Greenbelt Maryland

² Lab. d'Optique Atmos., CNRS, Univ. de Sciences et Techniques de Lille, Villeneuve d'Ascq, France

³ Service d' Aéronomie, Inst. Pierre Simon Laplace, Univ. Pierre de Marie Curie, 75252, Paris, France

experiment. It is shown that the product of the single scattering albedo, ω , and the phase function, P , for backscattering can be retrieved from the synergism between measurements avoiding *a priori* hypotheses required for inverting lidar measurements alone. The resultant value of $\omega P(180^\circ)=0.016\text{sr}^{-1}$ are significantly different from what is expected using Mie theory, but are in good agreement with recent results obtained from lidar observations of dust episodes. The inversion is robust in the presence of noise of 10% and 20% in the lidar signal in the 0.53 and 1.06 μm channels respectively. Calibration errors of the lidar of 5 to 10% can cause an error in optical thickness of 20 to 40% respectively in the tested cases. The lidar calibration errors cause degradation in the ability to fit the MODIS data. Therefore the MODIS measurements can be used to identify the calibration problem and correct for it. The CALIPSO-MODIS measurements of the profiles of fine and coarse aerosols, together with CALIPSO measurements of clouds vertical distribution, is expected to be critically important in understanding aerosol transport across continents and political boundaries, and to study aerosol-cloud interaction and its effect on precipitation and global forcing of climate.

1. Introduction

Analysis of the future spaceborne CALIPSO (Cloud-Aerosol Lidar and Infrared Pathfinder Satellite Observations) dual wavelength lidar data combined with spectral passive measurements from MODIS (Moderate resolution Imaging Spectroradiometer) will generate a data set combining the vertical profile information from CALIPSO with the detailed size information in the MODIS data. It is expected to resolve to a large extent the ambiguity in deriving the aerosol profile from the lidar measurements. There are several complementary differences between the way MODIS and CALIPSO observe aerosol. Over the oceans MODIS measures sunlight backscattered by the atmosphere in eight spectral channels from 0.41 μm to 2.1 μm . The MODIS short wavelengths are sensitive to scattering by both fine and coarse particles, while the long wavelengths are sensitive mainly to scattering by the coarse particles [Tanré et al 1997; Remer et al., 2001]. This information is used to derive the aerosol optical thickness separately for the fine and coarse aerosols.

Different physical processes control the formation and removal of the fine and coarse modes, defining a specific range for their size distributions in the atmosphere [Hopell et al. 1990]. The fine mode formed by condensation and oxidation of gases into liquids results in particles with effective radius mainly in the 0.1-0.25 μm range [Remer et al. 1998a, b; Dubovik et al., 2002]. Coarse particles, formed in physical processes have effective radius usually of 1 μm and larger [Dubovik et al., 2002]. Therefore in the inversion of the MODIS data we were able to use a limited set of aerosol sizes [Tanré et al., 1997] by imposing “real world” restrictions on the solutions, to narrow the range of the mathematical possibilities. We use a database of aerosol

size distributions derived from the Aerosol Robotic Network (AERONET) sun and sky measurements [Holben *et al.*, 1998; 2001; Dubovik *et al.* 2002] over the last 6 years from up to 100 stations world wide, to formulate the restrictions on the size distribution.

MODIS is sensitive to aerosols integrated on the entire atmospheric column and cannot resolve the aerosol profile. CALIPSO lidar will resolve the vertical distribution of the attenuated aerosol backscattering coefficients using two spectral channels at 0.53 and 1.06 μm . The narrower range of these wavelengths and the presence of only two cannot resolve a change in the size of the fine or coarse particles with a change in the concentration of the fine vs. coarse particles.

MODIS observations are for variety of scattering angles, while CALIPSO measurements are for a fixed scattering angle of 180° . The differences in the scattering angles and the difference in the sensitivity to aerosol properties (size, refractive index) of the MODIS and CALIPSO measurements makes the integrated data set of MODIS+CALIPSO lidar a powerful data base to resolve aerosol properties. Both CALIPSO satellite and MODIS on the Aqua satellite will fly in formation, observing the same spot on the ground within minutes.

Here we shall describe and test a procedure that combines active two wavelength backscattering lidar measurements from aircraft (simulating CALIPSO) with the passive spectral radiometer (MODIS) observations, keeping in mind that eventual integration with POLDER and lidar depolarization is expected to generate more refined results. This is one of the first attempts to invert simultaneously spaceborne active and passive measurements. Leon *et al.* (2002)

describes a different technique to invert passive and active measurements from space. The closest publication to our topic is probably the inversion of integrated ground based measurements of multispectral lidar data and profile spectral extinction coefficient derived from Raman lidar data reported by Müller et al., [1998] and Bockmann [2001]. However they did not use passive measurements and all observations were performed from the ground.

After a brief analysis of information content of MODIS and lidar data, we present the inversion scheme used for combining the two data sets. Data acquired during the SHADE campaign (Tanré et al., in preparation) are then used to show the feasibility of the inversion. Sensitivity and errors are discussed in the last section.

2. Information Content

A simple demonstration of the information content of the MODIS spectral channels, and their importance to the analysis of CALIPSO data is presented in Table 1. The aerosol radiance is the difference between the radiance at the top of the atmosphere with and without aerosol. A baseline model that contains both fine and coarse mode aerosol generates a given wavelength dependence between the lidar 0.53 and 1.06 μm channels. A change in the size of the fine or coarse mode particles from the baseline model can still give the same wavelength dependence between these two wavelengths by adjusting the relative concentration of the two modes. However the longer MODIS wavelengths (1.65 and 2.13 μm) can distinguish between these cases and resolve the ambiguity.

A statistical analysis of the spectral information in the lidar and MODIS data is based on the analysis of Tanré et al. [1996] for MODIS. It uses single scattering approximation for the aerosol radiance, L , at the top of the atmosphere ($L=C\tau\omega_0P$) for a range of fine and coarse aerosol modes. Here τ is the optical thickness, ω_0 , is the single scattering albedo and P the scattering phase function. C is proportionality constant. The weighting between the two modes is chosen to represent a specific spectral variation of the radiance $L(\lambda)$, expressed by an Ångström exponent function. For CALIPSO lidar wavelengths we can write:

$$\alpha_L(0.530/1.06) = - \ln[L(0.53)/L(1.06)] / \ln(0.53/1.06) \quad (1)$$

Figure 1 shows combinations of the fine and coarse modes that correspond to three fixed values of α_L : 0, 0.75 and 1.5. The figure shows that a wide range of effective radii falls into the same α_L category unresolved by the CALIPSO two wavelengths. It is better resolved by the MODIS wide spectral range, though the partial disorganization of the values of the effective radius for $\alpha_L = 0$ and to a smaller extend for $\alpha_L = 0.75$ shows also the limitation of the MODIS information content. The MODIS information on the aerosol size distribution depends also on the illumination and view directions [Tanré et al., 1996]. However we shall show that integration of MODIS and the lidar data can overcome even this limitation. It is concluded from Figure 1 that the use of the two lidar wavelengths can provide a first selection between modes and that the MODIS 2.1 μm can be used to define better the size distribution, however only for the entire atmospheric column.

3. Inversion scheme

From mathematical point of view, inversion of the integrated MODIS + CALIPSO lidar data still allows for many very different solutions. However in nature, not all of these solutions occur. The chosen aerosol sizes, shown in Table 2, do represent a simplification. They avoid mathematical solutions for effective radii around $0.5 \mu\text{m}$, that occur in nature only for clay particles that accompany in small quantities larger dust particles [Tanré *et al.*, 2001] and aged stratospheric aerosol that is sized just in between the fine and coarse modes [Kaufman *et al.*, 1994]. The result is a combination of 4 possible fine modes and 5 possible coarse modes that were selected to be used in the inversion of the MODIS data [Tanré *et al.*, 1997; Remer *et al.*, 2001]. Each mode represents a given aerosol scenario, from dry smoke, to wet urban pollution, salt and dust with refractive indices assigned accordingly. The approach was found to be very successful in the inversion of aircraft and MODIS data [Tanré *et al.*, 1999; Remer *et al.*, 2001]. Table 2 also gives the lidar backscattering ratio, $\omega P(180^\circ)$ calculated for each of the nine modes, to be used for lidar data inversion.

Inversion of the lidar and MODIS data is performed in two steps. First we invert the lidar data alone for all the possible combinations of the fine and coarse modes defined in Table 2. Since for each combination, the particle size distribution and refractive indices are defined in the table, and the lidar provides 2 pieces of information for each layer, and since we use calibrated lidar data, the inversion is well defined and proceeds using simple algebraic formulation. In other words, for a given combination of a fine (out of 4) and a coarse aerosol (out of 5) modes, the ambiguity in the inversion of the lidar data is removed and a unique profile of the optical thickness of the fine and

coarse modes is derived from the lidar data. The CALIPSO lidar data have two spectral channels. To obtain a unique solution, we assume that the atmospheric column is composed of only one fine aerosol mode, and one coarse mode in all the vertical layers. It is further assumed that the size of each of these modes does not vary with altitude, contrary to what one may expect from altitude variations of the relative humidity.

In the second step, the retrieved aerosol profiles for each of the 20 combinations are used to calculate 20 sets of MODIS spectral reflectances. Each of the 20 cases fits precisely the lidar data and the decision, which of the combinations is the proper one, is left to the MODIS measurements. The combination of a fine and a coarse mode that fits the MODIS measured spectral reflectances with minimal error is the winning combination. In the following we shall define the assumptions and mathematical steps in this procedure. The inversion procedure is described in the Appendix.

As a default the aerosol particles are assumed to be spherical, however as we know that for dust this is not valid we compensate partially for this assumption in the MODIS data inversion. We further test the limitations due to assumptions.

The look-up table uses the same aerosol models that are used in the MODIS inversion [Remer *et al.* 2001]. They include four fine modes with effective radius, R_{eff} , varying from 0.10 to 0.25 μm in step of 0.05 μm and five coarse modes, 3 for salt and 2 for dust with varying effective radii from 1 to 2.5 μm . Refractive indices are selected to fit the size of each mode, assuming that larger fine mode corresponds to higher relative humidity and smaller refractive

index. The lidar backscattering coefficient β_λ and the MODIS spectral radiance L_λ are computed for these models.

4. Application to SHADE data

The integrated CALIPSO-MODIS algorithm is applied to LEANDRE 1 lidar data collected by CNRS onboard the French Mystère-20 research aircraft during the Shade experiment off the West Africa coast (see Fig. 2 right panel) over the Northeastern Tropical Atlantic (Pelon et al., in preparation). The LEANDRE 1 system offers the same observational capability that the CALIPSO lidar (two channels at 0.53 and 1.06 μm and depolarization at 0.53 μm). We used here coincidental lidar and MODIS data within 20 minutes on Sept 26, 2000. Observations were acquired between the West coast of Africa and the Cape Verde archipelago. This location is well-known to be the main area of dust transport over the tropical Atlantic (Chiapello et al., 1997). The atmospheric aerosol is dominated by dust from the Sahara (Li et al., 1996). During summer time, the African dust is transported across the Atlantic in a dry and warm stable layer, the so-called Saharan air layer (SAL), located between 1.5 and 6 km in altitude (Prospero and Carlson, 1972). A conceptual model for the SAL has been proposed and validated by Karyampudi et al. (1999). This analysis shows that such a kind of dust transport occurs in September. During winter time, a low altitude transport of dust in the trade winds may prevail (Chiapello et al., 1995).

The lidar attenuated backscattering coefficient at 0.53 μm and the corresponding image of the MODIS derived optical thickness are shown in Fig. 2. They show the three dimensional structure of the dust layer. Examples of the MODIS spectral reflectance and the lidar profiles of the

attenuated backscattering coefficient at 0.53 and 1.06 μm are plotted in Fig. 3. The lidar backscattering attenuated coefficient is reported in 15 m resolution steps. The main dust layer is seen to extend up to 3 km in altitude, although the whole dust outbreak is seen to reach an upper altitude of 7-8 km. We averaged the data in non-equal steps based on the strength of the lidar signal. The averaged functions are shown by lines in the figure. The steps capture the main features of the return.

To invert dust data using LEANDRE 1 and MODIS measurements we have to account for the difference in the effects of non-sphericity on the scattering phase function. The MODIS data for the dust layer are for scattering angle of $\sim 135^\circ$ while the lidar return is analyzed for a scattering angle of 180° . For 135° scattering angle dust nonsphericity has a small impact on the scattering phase function [Mishchenko et al., 1997, Yang et al., 2000], much smaller than at 180° . Further multiple scattering for the high dust loading of Shade, reduces the effect of nonsphericity on the MODIS measurements but not as much on the lidar measurements. Multiple scattering impact on lidar data is expected to be of the order of a few per-cent as the radii of particles is not too large as compared to wavelength and as distance (about 10 km) is small (Eloranta, 1998). It is however expected to be larger for CALIPSO space-borne measurements (Winker et al., 2002). To account for the difference in the nonsphericity effect, we introduced a nonsphericity parameter, S_λ , that reduces the lidar spherical phase function at 0.53 μm and 1.06 μm . The parameter S_λ is determined at 0.53 μm and 1.06 μm as the value required for the lidar data to give column optical thicknesses of the fine and coarse aerosols that reproduce the MODIS measured spectral reflectances. MODIS derived optical thicknesses were found to be

accurate even in the presence of dust [Remer *et al.*, 2002]. The inversion procedure is based on the use of normalized parameters. Assuming nonsphericity effects are similar at both wavelengths, retrieval errors should be minimized. Therefore the parameter S_λ is expected to be a good approximate representation of the nonsphericity at 180° . We found that $S=0.42$ and 0.43 at 0.53 and $1.06 \mu\text{m}$, respectively, gives a good fit to the MODIS data (see left panel of Fig. 4) with residual error of 3.6%, for model 6. An error of 2-4% in the MODIS spectral reflectances is expected due to small uncertainty in the MODIS calibration (1-2%) and uncertainty in the ocean surface reflectance. The validity of taking into account nonsphericity as a factor S is further confirmed by the fact that values of S retrieved at both wavelengths are identical. The value $S=0.42$ gives is similar to calculations of the ratio of phase function of spheroids to spheres for size parameter X of 15 to 25 that corresponds to dust with effective radius of $2 \mu\text{m}$. For $S \leq 0.40$ or $S \geq 0.45$ the difference between MODIS and LEANDRE 1 lidar nonsphericity is large enough so that there is no value of optical thickness that can satisfy both the LEANDRE 1 and MODIS measurements. The right panel of Fig. 4 shows the profiles of the extinction coefficient of the fine and coarse particles for the optimum solution ($S=0.42$) and for the other values of S .

Inversion products of the lidar and MODIS data of Fig. 3 are shown in Fig. 5. Note that correction of the attenuation of the backscattering function by the aerosol layers in the inversion process shifts the maximum extinction of the coarse mode from 3 to 2 km. The lidar ratio derived in this inversion at both wavelengths is 63 ± 6 sr. It was increased from 30 sr by the nonsphericity correction. This value is in good agreement with the one derived from lidar data analysis (Pelon

et al., in preparation) and with values recently found from ground-based Raman lidar measurements (Mattis et al., 2002).

5. Sensitivity to calibration errors and noise in the lidar data

What is the sensitivity of the inversion to calibration errors and noise in the lidar data? In the following we discuss the sensitivity with the help of the dust data from the SHADE experiment. In Fig. 6 we check the sensitivity of the inversion to the lidar calibration. It is expected that the satellite lidar data will be more noisy than the aircraft lidar, due to the larger distance of 700 kms vs. 8 kms from the dust layer. Noise in the lidar system may cause errors in the absolute lidar calibration. We tested both cases with same or different calibration errors in the two channels. A profile of attenuated backscattering coefficient was chosen and an error in calibration of 5% in both channels was introduced. The calibration errors introduce an error of 20% in the column optical thickness. However the fit to MODIS data had an unrealistic high value of 9%, an indicator of inconsistency between the lidar and MODIS data, due to the calibration errors. Note that the inversion process can find the nonsphericity parameter S only if the calibration is well known as in this case of aircraft lidar data. Double calibration error (10%) doubles the error in the optical thickness and farther increases the error in fitting the MODIS data to 16% - a clear indicator of the lidar calibration errors.

Introduction of noise to the lidar data has a much smaller effect on the inversion than systematic calibration errors. We added random errors to the lidar backscattering profile using the transformation:

$$\beta_{\lambda} \rightarrow \beta_{\lambda}(1+rC_N/100\%)$$

where r is a random number between -1 and $+1$ and C_N is the magnitude of the noise, 10% at $\lambda=0.53 \mu\text{m}$ and 20% at $\lambda=1.06 \mu\text{m}$. Profiles of the inverted extinction coefficient (Fig. 7) show that the noise did not change the fundamental properties of the derived aerosol layer. The differences are larger for the fine mode due to its small contribution to the optical thickness in this case. Addition of the noise did not have a systematic effect on the column properties. It changed the column optical thickness at $0.53 \mu\text{m}$ from 0.87 to 0.85 ± 0.1 . The fraction of the fine mode in the optical thickness increased from 0.11 to 0.14 ± 0.08 . The inversion process identified the same modes of the fine and coarse particles 80% of the time. A histogram of the optical thicknesses derived in 46 calculations with random noise is shown in Fig. 8.

6. Conclusions

Combined inversion of the MODIS spectral radiances with the CALIPSO 2 wavelength profiles of the attenuated backscattering coefficient, takes advantage of the wide MODIS spectral range and the vertical profile information in the lidar data. The inversion produces the vertical profiles of the fine and coarse mode. In case the size of the fine or coarse modes vary as a function of height, the inversion will choose the average size to represent the column. The inversion was shown to be sensitive to the data quality. Introduction of calibration errors into the lidar data or the presence of nonsphericity is not compensated by a different aerosol profile but rather results in large and unacceptable retrieval errors. This feature can be used to improve the calibration of the lidar or the MODIS instrument, or improve the aerosol model. Application to the SHADE data over heavy dust from Africa resulted as expected in profile of mainly dust, in agreement with in situ measurements [Leon et al., 2002].

Further improvement in the analysis is expected from additional synergism. The PARASOL mission with a POLDER instrument on board will be part of the same train as AQUA and CALIPSO satellites. It will take passive measurements of the two dimensional polarized radiation field in five spectral channels in the 0.44-0.91 μm range and for wide range of view zenith angles and all azimuth directions [Deuze, et al., 2000]. This information when integrated into the MODIS+CALIPSO data will further constrain the inversion. POLDER also measures the light polarization and CALIPSO measures the depolarization profile, both helping to distinguish spherical particles from non-spherical ones and in case of POLDER adding sensitivity to the particle refractive index not derived from the MODIS data. Polarization is also expected to constrain better the size of the fine mode.

References

- Bockmann, C., Hybrid regularization method for the ill-posed inversion of multi-wavelength lidar data in the retrieval of aerosol size distributions, *Appl. Optics*, **40**, 1329-1342 (2001)
- Chiapello, I., G. Bergametti, B. Chatenet, P. Bousquet, F. Dulac, and E. Santos Soares, Origins of African dust transported over the northeastern tropical Atlantic., *J. Geophys. Res.*, **102** (D12), 13701-13709, 1997.
- Chiapello, I., G. Bergametti, L. Gomes, B. Chatenet, F. Dulac, J. Pimenta, and E. Santos Soares, An additional low layer transport of Sahelian and Saharan dust over the north-eastern tropical Atlantic., *Geophys. Res. Lett.*, **22** (23), 3191-3194, 1995.
- Deuzé, J.-L. *et al.* Estimate of the aerosol properties over the ocean with POLDER. *J. Geophys. Res.* **105**, 15329-15346 (2000).

- Dubovik, O., B.N. Holben, T. F. Eck, et al., Climatology of aerosol absorption and optical properties in key worldwide locations, *J. Atmos. Sci.*, **59**, 590-608, 2002.
- Eloranta, E. W. Practical model for the calculation of multiply scattered lidar returns, *Appl. Opt.*, **37**, 2464-2472, 1998
- Holben, B. N., T. F. Eck, I. Slutsker, D. Tanré, J. P. Buis, A. Setzer, E. Vermote, J. A. Reagan, Y. J. Kaufman, T. Nakajima, F. Lavenue, I. Jankowiak and A. Smirnov: AERONET-A federated instrument network and data archive for aerosol characterization, *Rem. Sens. Environ.*, **66**, 1-16, 1998.
- Holben B. N., D. Tanre, A. Smirnov et al., An emerging ground-based aerosol climatology: Aerosol optical depth from AERONET, *J. Geophys. Res.*, **106**, 12067-12097, 2001
- Hoppel, W. A. *et al.* Aerosol size distribution and optical properties found in the marine boundary layer over the Atlantic Ocean. *J. Geophys. Res.* **95**, 3659–3686 (1990).
- Karyampudi, V.M., S.P. Palm, J.A. Reagen, H. Fang, W.B. Grant, R.M. Hoff, C. Moulin, H.F. Pierce, O. Torres, E.V. Browell, and S.H. Melfi, Validation of the saharan dust plume conceptual model using lidar, Meteosat, and ECMWF data, *Bull. Amer. Meteor. Soc.*, **80**, 1045-1075, 1999.
- Kaufman, Y. J., A. Gitelson, A. Karnieli, et al., Size Distribution and Scattering Phase Function of Aerosol Particles Retrieved from Sky Brightness Measurements. *J. Geophys. Res.*, **99**, 10341-10356 (1994)
- Leon, J. F., D. Tanré, J. Pelon and Y. J. Kaufman, Characterization of tropospheric aerosols based on active and passive remote sensing synergy, submitted to JGR Shade special issue, 2002

- Li, X., H. Maring, D. Savoie, K. Voss, and J.M. Prospero, Dominance of mineral dust in aerosol scattering in the North Atlantic trade winds, *Nature*, **380**, 416-419, 1996.
- Mishchenko, M. I., L. D. Travis, R. A. Kahn, R. A. West, Modeling phase functions for dustlike tropospheric aerosols using a shape mixture of randomly oriented polydisperse spheroids *J. Geophys. Res.*, **102**, 16831-16847, 1997.
- Müller D, U. Wandinger, D. Althausen et al., Retrieval of physical particle properties from lidar observations of extinction and backscatter at multiple wavelengths, *Appl. Optics*, **37**, 2260-2263 (1998).
- Prospero, J. M., and T. N. Carlson, Vertical and areal distribution of Saharan dust over the western equatorial north Atlantic Ocean., *J. Geophys. Res.*, **77** (27), 5255-5265, 1972.
- Remer, L. A. and Y. J. Kaufman, Dynamical aerosol model: Urban/industrial aerosol., *J. Geophys. Res.*, **103**, 13,859-13,871 (1998a)
- Remer, L. A., Y. J. Kaufman, B. N. Holben, et al., Tropical biomass burning smoke aerosol size distribution model. *J. Geophys. Res.*, **103**, 31,879-31,892 (1998b).
- Remer, L. A., D. Tanré, Y. J. Kaufman, et al., Validation of MODIS Aerosol Retrieval Over Ocean, submitted to *Geoph. Res. Lett.* (2002).
- Remer, L. A., D. Tanré, Y. J. Kaufman, C. Ichoku, S. Mattoo, R. Levy, D. A. Chu, B. N. Holben, J. V. Martins, and R.-R. Li and Z. Ahmad, Validation of MODIS Aerosol Retrieval Over Ocean, accepted to *GRL* 2001
- Tanré, D., M. Herman and Y.J. Kaufman, Information on aerosol size distribution contained in solar reflected radiances, *J. Geophys. Res.*, **101**, 19043-19060 (1996).
- Tanré, D., Y. J. Kaufman, M. Herman and S. Mattoo, Remote sensing of aerosol over oceans from EOS-MODIS. *J. Geophys. Res.* **102**, 16971-16988 (1997).

Tanré, D., Y. J. Kaufman, B.N. Holben, B. Chatenet, A. Karnieli, F. Lavenu, L. Blarel, O.

Dubovik, L.A. Remer, A. Smirnov: Climatology of dust aerosol size distribution and optical properties derived from remotely sensed data in the solar spectrum, *J. Geophys. Res.*, **106**, 18205-18217, 2001

Tanré, D., L.R. Remer, Y.J. Kaufman et al., Retrieval of Aerosol Optical Thickness and Size Distribution Over Ocean from the MODIS Airborne Simulator during Tarfox, *J. Geophys. Res.*, **104**, 2261-2278 (1999).

Yang, P, K. N. Liou, M. I. Mishchenko, B. C. Gao, Efficient finite-difference time-domain scheme for light scattering by dielectric particles: application to aerosols, *Appl. Opt.*, **39**, 3727-3737, 2000.

Winker et al., 2002

Appendix: Inversion Scheme

In this appendix we describe the inversion process of the MODIS spectral radiances in the 0,55-2.13 μm range together with the CALIPSO 2 wavelength (0.53 and 1.06 μm) lidar

The lidar backscattering coefficient is defined by:

$$\beta_{\lambda} = C_L \omega_{\lambda} P_{\lambda}(180) \Delta\tau_{\lambda}.$$

We define a normalized backscattering coefficient, that does not depend on the aerosol optical thickness, $\beta^*_{\lambda} = \beta_{\lambda} / \Delta\tau_{0,53}$, where $\Delta\tau_{0,53}$ is the optical thickness of the layer:

$$\beta^*_{\lambda} = C_L \omega_{\lambda} P_{\lambda}(180) \Delta\tau^*_{\lambda} \tag{A1}$$

where $\Delta\tau^*_{1.06} = \Delta\tau_{1.06} / \Delta\tau_{0.53}$ and $\Delta\tau^*_{0.53} = 1$. The coefficient C_L defines the lidar properties and is used as $C_L = 1$ in the simulation.

Step 1: Inversion of the CALIPSO data

For each combination of a fine “f” and a coarse “C” mode, the two wavelength backscattering coefficient measured by the lidar and received from each layer “i” are inverted starting from the top of the atmosphere. For the top layer in the atmosphere, $i=1$, the CALIPSO measurements, $\beta_{m\lambda,1}$, are simply the backscattering coefficients at $\lambda=0.53$ and $\lambda=1.06 \mu\text{m}$. For lower layers the measurements are the attenuated backscattering coefficients by the layers above. For the top layer the spectral ratio ξ_{m1} ,

$$\xi_{m1} = \beta'_{m1.06,1} / \beta'_{m0.53,1} \quad (\text{A2})$$

is calculated after subtracting Rayleigh backscattering, $\beta_{R\lambda,1}$, and accounting for Rayleigh attenuating due to higher layers.

$$\beta'_{m\lambda,1} = \beta_{m\lambda,1} \exp(2 * \Delta\tau_R) - \beta_{R\lambda,1} \quad (\text{A3})$$

$\beta_{R\lambda,1}$ is the Rayleigh unattenuated backscattering coefficient

It is sensitive to the aerosol size but not to the aerosol concentration. Once the aerosol model is determined by the inversion process, the phase function and the single scattering albedo can be recomputed and used together with the backscattering coefficients at $\lambda=0.53$ to derive the optical thickness.

The ratio ξ_{m1} , is used to determine the contribution of the fine mode in layer $i=1$ to the aerosol optical thickness at $0.53 \mu\text{m}$, η_1 . The aerosol backscattering coefficients $\beta'_{m\lambda,1}$ is combined from a fraction, η_1 of the fine mode backscattering and fraction $(1-\eta_1)$ of the coarse mode backscattering:

$$\beta'_{m\lambda,1} = \eta_1 \beta'_{m\lambda,1,f} + (1-\eta_1) \beta'_{m\lambda,1,c} \quad (\text{A4})$$

From Eqs. A1-A4 we can extract the expressions for η_1 and $\Delta\tau_\lambda$. First we calculate η_1 from the measured ratio ξ_m using the normalized backscattering coefficients for unit optical thickness at $0.55 \mu\text{m}$ ($\Delta\tau^*_{0.53}=1$) stored in the lookup table by inverting eqs. A2 and A3:

$$\eta_1 = [\beta^*_{1.06,1,c} - \xi_{m1} \beta^*_{0.53,1,c}] / [\xi_{m1} \beta^*_{0.53,1,f} - \xi_{m1} \beta^*_{0.53,1,c} - \beta^*_{1.06,1,f} + \beta^*_{1.06,1,c}] \quad (\text{A5})$$

Then we derive the optical thickness of the layer - $\Delta\tau_{0.53}$ and $\Delta\tau_{1.06}$ from the measured backscattering coefficient $\beta'_{m\lambda,1}$ and the definitions (Eq. A1):

$$\Delta\tau_{0.53} = \beta'_{m0.53,1} / \beta^*_{0.53,1} \quad \text{and} \quad \Delta\tau_{1.06} = \Delta\tau_{0.53} \Delta\tau^*_{1.06} \quad (\text{A6})$$

where the functions $\beta^*_{0.53,1}$ and $\Delta\tau^*_{1.06}$ for the combined fine and coarse aerosol are obtained from the look up table:

$$\beta^*_{0.53,1} = \eta_1 \beta^*_{0.53,1,f} + (1-\eta_1) \beta^*_{0.53,1,c} \quad \text{and} \quad \Delta\tau^*_{1.06} = \eta_1 \Delta\tau^*_{1.06,1,f} + (1-\eta_1) \Delta\tau^*_{1.06,1,c}$$

The results of the inversion for the top layer ($i=1$) are η_1 , $\Delta\tau_{0.53,1}$ and $\Delta\tau_{1.06,1}$.

For lower layers, $i > 1$, the backscattering coefficients are attenuated by the layers above: layers 1 through $i-1$. Since the measured attenuated backscattering coefficient for the layer i , $\beta_{m\lambda,i}$ is related to the non-attenuated aerosol backscattering coefficient in the layer - $\beta'_{m\lambda,i}$, by:

$$\beta_{m\lambda,i} = [\beta'_{m\lambda,i} + \beta_{R\lambda,i}] \exp(-2\tau_{\lambda,i}) \text{ therefore: } \beta'_{m\lambda,i} = \beta_{m\lambda,i} \exp(2\tau_{\lambda,i}) - \beta_{R\lambda,i} \quad (\text{A7})$$

Where $\tau_{\lambda,i}$ is the combined aerosol and Rayleigh optical thickness from the top of the atmosphere to layer "i":

$$\tau_{\lambda,i} = \Delta\tau_{\lambda,1} + \dots + \Delta\tau_{\lambda,i-1} + \tau_{R\lambda,i} \quad (\text{A8})$$

and $\tau_{R\lambda,i}$ is the Rayleigh optical thickness from top of atmosphere down to layer i . With this transformation we can apply the same formulation as to the top layer (eqs. A4 and A5), replacing "1" with "i" and resulting in η_i , $\Delta\tau_{0.53,i}$:

$$\eta_i = [\beta_{1.06,i,c}^* - \xi_{mi} \beta_{0.53,i,c}^*] / [\xi_m \beta_{0.53,i,f}^* - \xi_m \beta_{0.53,i,c}^* - \beta_{1.06,i,f}^* + \beta_{1.06,i,c}^*] \text{ and } (\text{A5i})$$

$$\Delta\tau_{0.53} = \beta_{m\lambda,i} / [\beta_{\lambda,i,f}^* \eta_i + \beta_{\lambda,i,c}^* (1 - \eta_i)] \quad (\text{A6i}).$$

Not every mode combination will give a physical solution. Unphysical solution will be reflected in values of η_i larger than 1.0 or negative. If the value of η_i is $\eta_i > 1.2$ or $\eta_i < -0.2$, the solution for this mode combination is void, otherwise it is rounded to 1.0 and 0.0 respectively.

Step 2: Use of MODIS spectral data

Inversion of the CALIPSO data resulted in up to 20 different combinations of fine and coarse aerosol profiles, all of them reproducing the lidar profiles of the attenuated backscattering coefficient at 0.53 and 1.06 μm . In step 2, the MODIS measured spectral radiance $L_{m\lambda\text{MOD}}$ is used to choose the best solution between these 20. For each of the combinations of the fine, “f”, and coarse, “C” modes inversion of the lidar data resulted in $\eta_{i,f,C}$, $\Delta\tau_{0.53,i,f,C}$, for layer “i”. The column total optical thickness $\tau_{0.53,f,C}$ and the contribution of the fine mode in the entire column, $\eta_{f,C}$ is then,

$$\tau_{0.53,f,C} = \sum \Delta\tau_{0.53,i,f,C}, \eta_{f,C} = [\sum (\eta_{i,f,C} \Delta\tau_{0.53,i,f,C})] / \tau_{0.53,f,C} \quad (\text{A9})$$

For each “f” and “C” with corresponding $\tau_{0.53,f,C}$ and $\eta_{f,C}$, a unique MODIS spectral radiance - $L_{\lambda\text{MOD},f,C}$ is calculated and compared with the measured MODIS radiance - $L_{m\lambda\text{MOD}}$. A minimum error $\epsilon_{f,C}$ [Tanré et al 1997]:

$$\epsilon_{f,C} = (1/6) [\sum_{\lambda} (L_{\lambda\text{MOD},f,C} - L_{m\lambda\text{MOD}})^2 / (L_{m\lambda\text{MOD}})^2]^{0.5} \quad (\text{A10})$$

is used to choose the best combination “f” and “C” with corresponding profiles η_i , $\Delta\tau_{0.53,i}$ and $\Delta\tau_{1.06,i}$. The summation is on the 6 MODIS channels 0.55-2.1 μm .

Table 1: Example of 4 aerosol size distributions, that give the same spectral dependence of the aerosol reflected radiance between 0.53 μm and 1.06 μm and different radiance at 2.1 μm . The radiance is normalized to 1.0 at 0.55 μm and shown for 1.06 and 2.13 μm . The aerosol size distribution is composed of 2 log-normal modes, fine and coarse, with effective radius R_{eff} given in the table. The effective radius and % contribution of each mode to the optical thickness at 0.53 μm defines the normalized spectral optical thickness in the whole solar spectrum.

| Fine mode | | Salt mode | | Aerosol radiance $\alpha_{\lambda}(0.53,$ | | |
|---------------------|---------------------|---------------------|---------------------|---|--------------------|----------------------|
| Reff, μm | Contri- bution % | Reff, μm | Contri- bution % | 1.06 μm | 2.13 μm | 1.06 μm) |
| 0.15 | 50 | 1 | 50 | 0.693 | 0.357 | 0.53 |
| 0.2 | 60 | 1 | 40 | 0.69 | 0.331 | 0.54 |
| 0.25 | 69 | 1 | 31 | 0.689 | 0.309 | 0.54 |
| 0.2 | 63 | 1.5 | 37 | 0.697 | 0.4 | 0.52 |

Table 2: Aerosol Models for the fine and coarse modes used to retrieve the aerosol properties from the integrated CALIPSO and MODIS data set. R_g and σ are the median radius and standard deviation of the log-normal size distribution. R_{eff} is the effective radius of the distribution: $R_{eff} = R_g \exp(2.5\sigma^2)$. The value of the lidar backscattering ratio, $\omega P(180^\circ)$, is also given.

fine particles:

| | $\lambda=0.55-->0.86\mu\text{m}$ | $\lambda=1.24\mu\text{m}$ | $\lambda=1.64\mu\text{m}$ | $\lambda=2.13\mu\text{m}$ | R_g | σ | R_{eff} | $\omega P(180^\circ)$ at 0.55 μm | Comments |
|---|----------------------------------|---------------------------|---------------------------|---------------------------|-------|----------|-----------|---|-------------------|
| 1 | 1.45-0.0035i | 1.45-0.0035i | 1.43-0.01i | 1.40-0.005i | 0.07 | 0.40 | 0.10 | 0.28 | Small fine |
| 2 | 1.45-0.0035i | 1.45-0.0035i | 1.43-0.01i | 1.40-0.005i | 0.06 | 0.60 | 0.15 | 0.20 | Intermediate fine |
| 3 | 1.40-0.0020i | 1.40-0.0020i | 1.39-0.005i | 1.36-0.003i | 0.08 | 0.60 | 0.20 | 0.17 | Wet large fine |
| 4 | 1.40-0.0020i | 1.40-0.0020i | 1.39-0.005i | 1.36-0.003i | 0.10 | 0.60 | 0.25 | 0.17 | Wetter large fine |

coarse particles:

| | $\lambda=0.55-->0.86\mu\text{m}$ | $\lambda=1.24\mu\text{m}$ | $\lambda=1.64\mu\text{m}$ | $\lambda=2.13\mu\text{m}$ | R_g | σ | R_{eff} | $\omega P(180^\circ)$ at 0.55 μm | comments |
|---|--|---------------------------|---------------------------|---------------------------|-------|----------|-----------|---|-------------------|
| 5 | 1.45-0.0035i | 1.45-0.0035i | 1.43-0.0035i | 1.43-0.0035i | 0.40 | 0.60 | 0.98 | 0.44 | Wet Sea salt type |
| 6 | 1.45-0.0035i | 1.45-0.0035i | 1.43-0.0035i | 1.43-0.0035i | 0.60 | 0.60 | 1.48 | 0.44 | Wet Sea salt type |
| 7 | 1.45-0.0035i | 1.45-0.0035i | 1.43-0.0035i | 1.43-0.0035i | 0.80 | 0.60 | 1.98 | 0.41 | Wet Sea salt type |
| 8 | 1.53-0.001i at 0.55-0.86 μm | 1.46-0.000i | 1.46-0.001i | 1.46-0.000i | 0.60 | 0.60 | 1.48 | 0.96 | Dust-like type |
| 9 | 1.53-0.001i at 0.55-0.86 μm | 1.46-0.000i | 1.46-0.001i | 1.46-0.000i | 0.50 | 0.80 | 2.50 | 0.92 | Dust-like type |

Figure Captions:

Fig. 1: The spectral normalized aerosol radiance (normalized by the value at $0.53 \mu\text{m}$) for a range of combinations of the aerosol fine and coarse modes that result in 3 specific values of the spectral slope α_L . For each case the effective radius R_{eff} of the whole size distribution is shown. MODIS $2.1 \mu\text{m}$ channel resolves most of the differences among the different cases.

Fig. 2: Left - lidar returns at $0.53 \mu\text{m}$ as a function of longitude, showing the presence of dust at 2-3 km altitude. On the right the MODIS image of the derived aerosol optical thickness is shown. Red colors correspond to high aerosol concentration. The lidar path is shown in the MODIS image by black line.

Fig. 3: Left – profiles of the attenuated lidar backscattering coefficient at $0.53 \mu\text{m}$ (green) and $1.06 \mu\text{m}$ (red). The measured lidar returns, integrated on 15 m altitude are given by dots. The data were averaged every in non-equal steps shown by the lines. Right – corresponding MODIS spectral reflectances measured over the ocean at the top of the atmosphere, outside the ocean glint.

Fig. 4: Sensitivity of the inversion of LEANDRE1 + MODDIS data to the nonsphericity parameter - S. In the inversion process, the lidar backscattering phase function associated with coarse particles was multiplied by S. The left figure shows the error in fitting the MODIS spectral reflectance (black line), and the aerosol optical thickness (green) and fraction of fine particles contribution to the optical thickness (red) that resulted from the inversion. For $S=0.42$ there is

sharp decline in the error on both sides of $S=0.42$. For this value the fraction contribution of the fine mode is small (11%) as expected for the dust episode.

Fig. 5: Results of inversion of the lidar profiles and MODIS spectra of Fig. 4. Note that the maximum extinction occurs in lower altitude than the maximum backscattering coefficient due to its attenuation by the aerosol above the given layer..

Fig. 6: Sensitivity of the inversion of the lidar profiles to errors in calibration of 5% to 10% in each or both of the channels as indicated. The heavy line shows the solution with no additional errors. The values of the column optical thickness of the fine (τ_f) and coarse (τ_c) aerosols are given in the figure.

Fig. 7: Profiles of the extinction coefficient obtained for the original data (solid thick lines) and in the presence of random noise in the backscattering coefficient of 10% at $0.53 \mu\text{m}$ and 20% at $1.06 \mu\text{m}$ (thin lines with symbols). Fine mode is shown by red and coarse mode by green.

Fig. 8: Histogram of the column aerosol optical thickness obtained in the presence of random noise in the backscattering coefficient of 10% at $0.53 \mu\text{m}$ and 20% at $1.06 \mu\text{m}$. The yellow line is the solution without the noise.

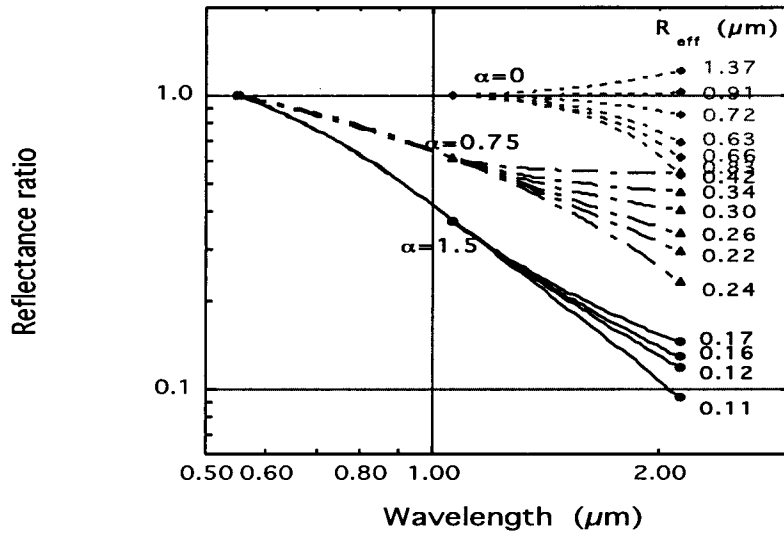


Fig. 1: The spectral normalized aerosol radiance (normalized by the value at 0.53 μm) for a range of combinations of the aerosol fine and coarse modes that result in 3 specific values of the spectral slope α_L . For each case the effective radius R_{eff} of the whole size distribution is shown. MODIS 2.1 μm channel resolves most of the differences among the different cases.

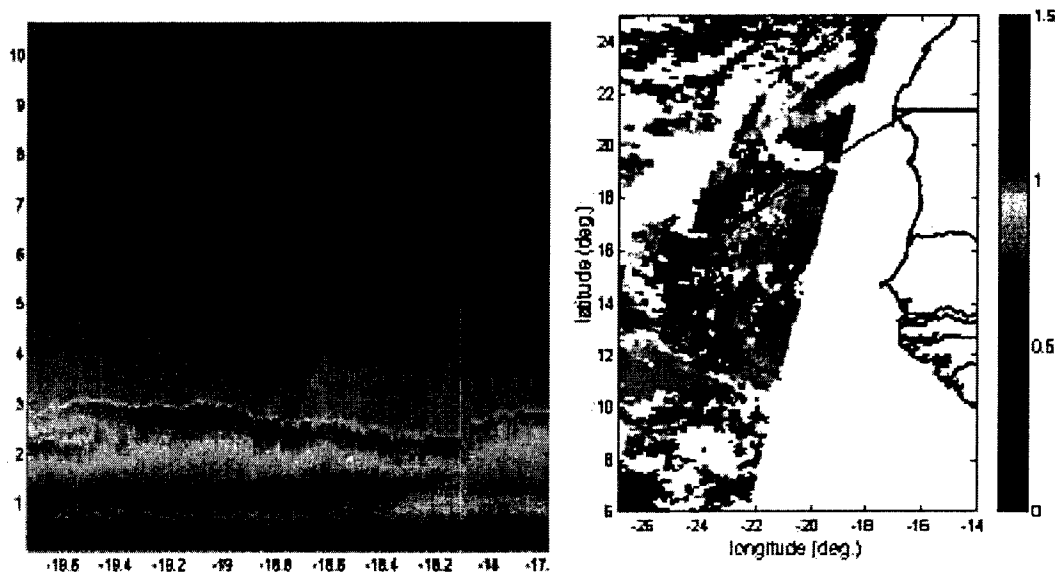


Fig. 2: Left - lidar returns at $0.53 \mu\text{m}$ as a function of longitude, showing the presence of dust at 2-3 km altitude. On the right the MODIS image of the derived aerosol optical thickness is shown. Red colors correspond to high aerosol concentration. The lidar path is shown in the MODIS image by black line.

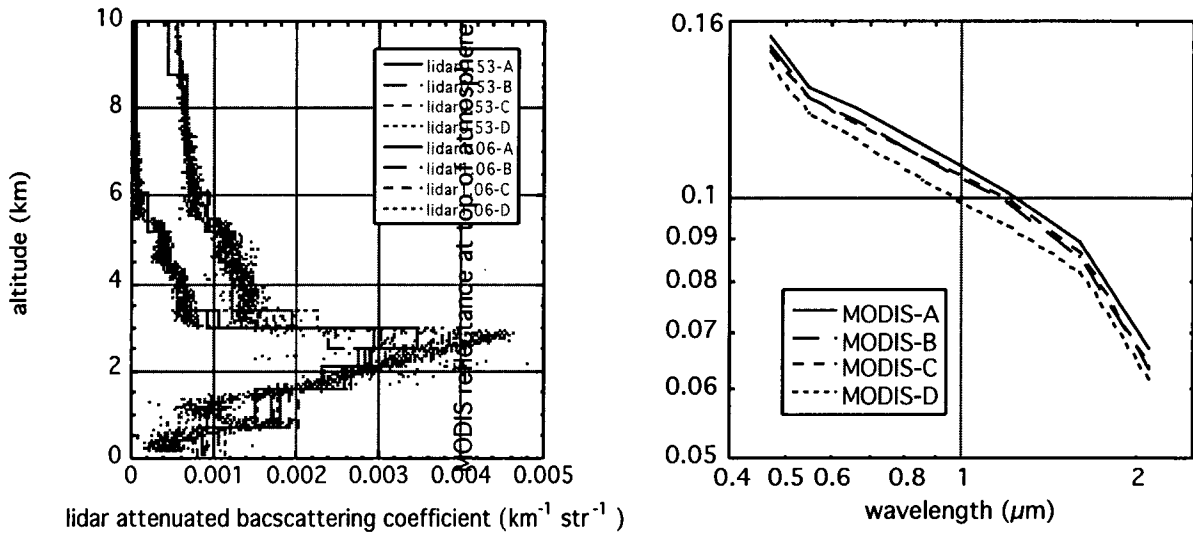


Fig. 3: Left – profiles of the attenuated lidar backscattering coefficient at 0.53 μm (green) and 1.06 μm (red). The measured lidar returns, integrated on 15 m altitude are given by dots. The data were averaged every in non-equal steps shown by the lines. Right – corresponding MODIS spectral reflectances measured over the ocean at the top of the atmosphere, outside the ocean glint.

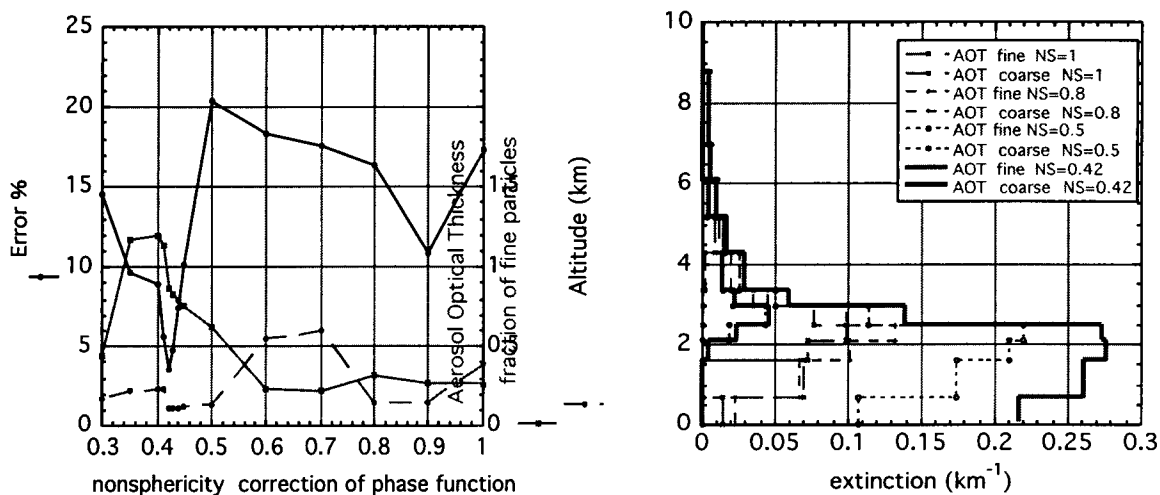


Fig. 4: Sensitivity of the inversion of Calipso+MODDIS data to the nonsphericity parameter - S.

In the inversion process, the lidar backscattering phase function associated with coarse particles was multiplied by S. The left figure shows the error in fitting the MODIS spectral reflectance (black line), and the aerosol optical thickness (green) and fraction of fine particles contribution to the optical thickness (red) that resulted from the inversion. For S=0.42 there is sharp decline in the error on both sides of S=0.42. For this value the fraction contribution of the fine mode is small (11%) as expected for the dust episode.

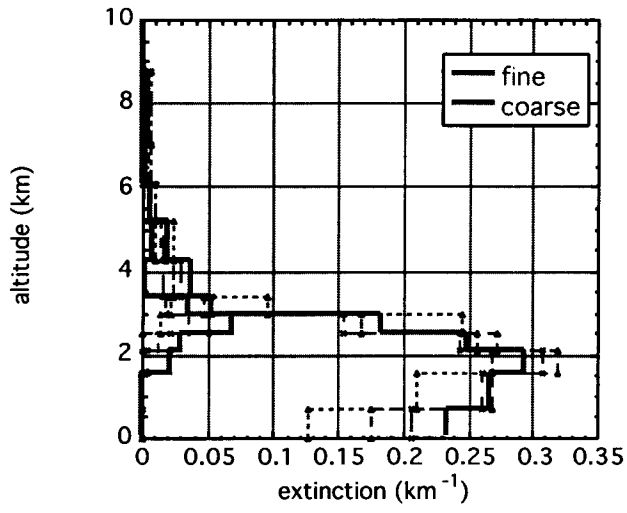


Fig. 5: Results of inversion of the lidar profiles and MODIS spectra of Fig. 4. Note that the maximum extinction occurs in lower altitude than the maximum backscattering coefficient due to its attenuation by the aerosol above the given layer.

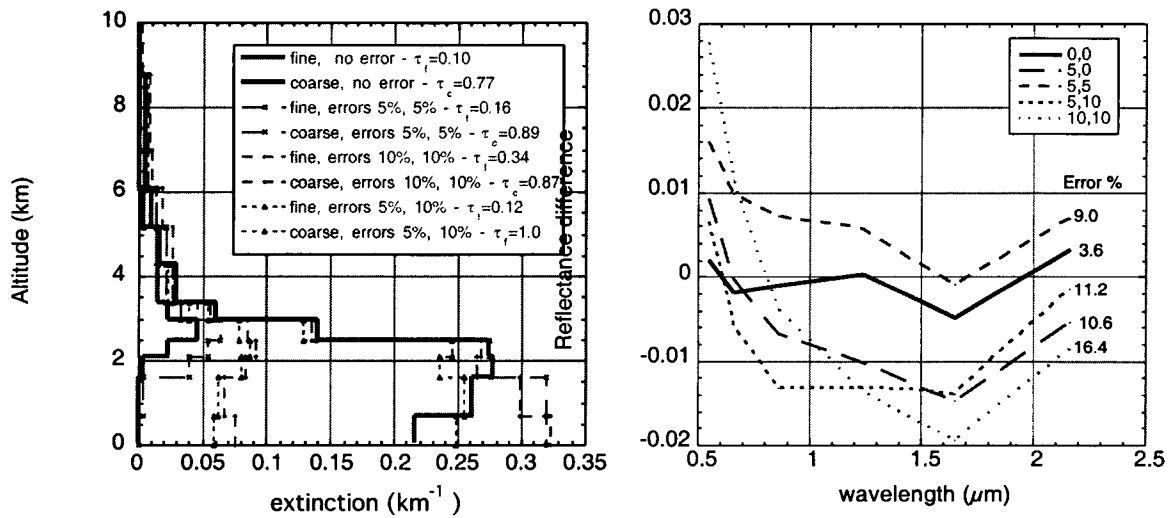


Fig. 6: Sensitivity of the inversion of the lidar profiles to errors in calibration of 5% to 10% in each of both of the channels as indicated. Right: profile of the extinction coefficients. The heavy line shows the solution with no additional errors. The values of the column optical thickness of the fine (τ_f) and coarse (τ_c) aerosols are given in the figure. Left: Spectra of the reflectance difference between the derived solution and the MODIS measurements.

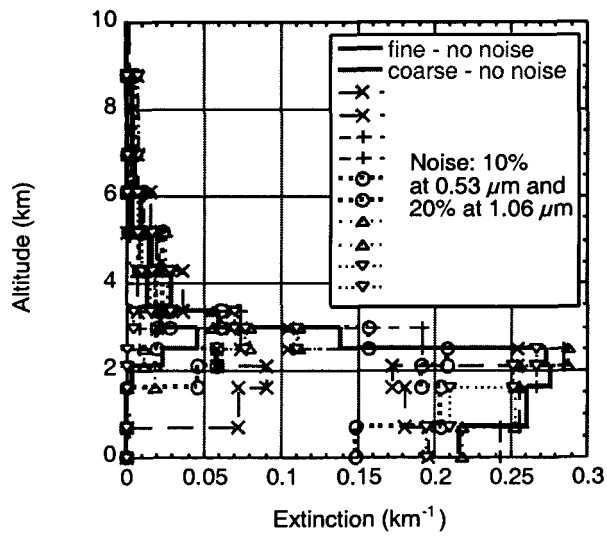


Fig. 7: Profiles of the extinction coefficient obtained for the original data (solid thick lines) and in the presence of random noise in the backscattering coefficient of 10% at $0.53 \mu\text{m}$ and 20% at $1.06 \mu\text{m}$ (thin lines with symbols). Fine mode is shown by red and coarse mode by green.

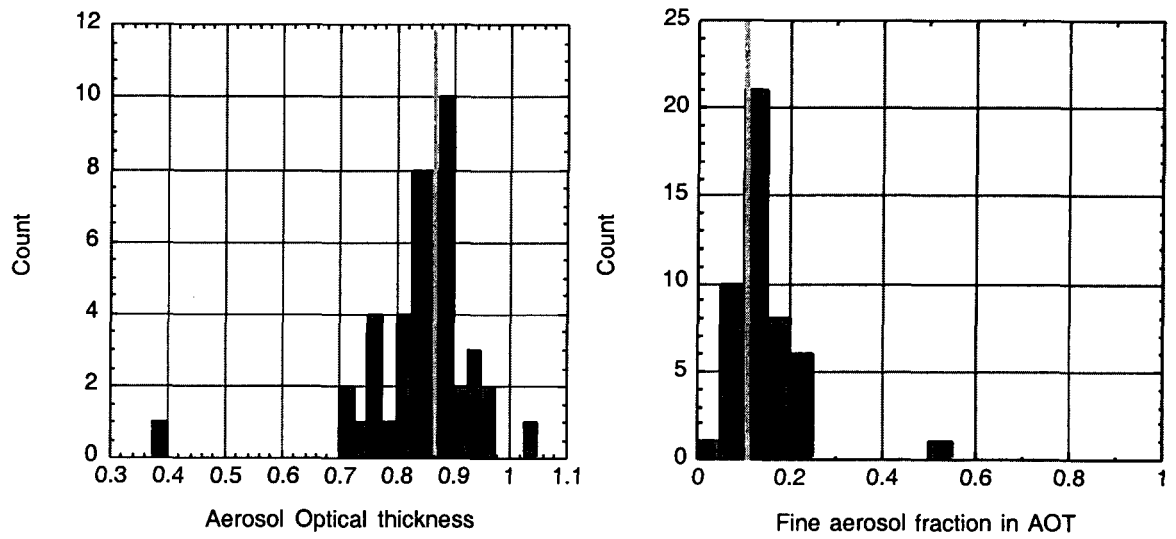


Fig. 8: Histogram of the column aerosol optical thickness (left) and fine aerosol fraction (right) obtained in the presence of random noise in the backscattering coefficient of 10% at $0.53 \mu\text{m}$ and 20% at $1.06 \mu\text{m}$. The yellow line is the solution without the noise.

Retrievals of profiles of fine and coarse aerosols using lidar and radiometric space measurements

Submitted to IEEE: TGRS-00230-2002

Yoram Kaufman, Didier Tanré, Jean-François Léon and Jacques Pelon

Popular summary

In the next couple of years we shall see the launch of the first lidars into space, designed to observe the distribution with height of dust, air pollution and smoke aerosols. Lidars send pulses of light and detect the strength of reflection and distance of small mirrors – dust smoke or air pollution aerosols that reflect the light. Though the aerosol layers can be easily detected from the lidar data, their exact height distribution and size cannot be derived from the lidar data alone. In this paper we show that combination of the Calipso lidar data with observations from MODIS contains enough information about the aerosol so that we can distinguish between the vertical distribution of dust and smoke or air pollution and sea salt aerosols. The new method was applied to measurements from MODIS and airborne lidar of a dust storm off the coast of West Africa during the SHADE experiment. The results show the presence of a dust layer centered at 2 km, and a thin layer of air pollution centered at 3 km.